

PAPER • OPEN ACCESS

Machine learning phases in swarming systems

To cite this article: Tingting Xue *et al* 2023 *Mach. Learn.: Sci. Technol.* 4 015028

View the [article online](#) for updates and enhancements.

You may also like

- [In Situ Measurement of the Conductance of Regioregular Poly-3,4-didodecyl-2,2':5,2'-terthiophene during Potentiodynamic Growth](#)

Daniilo Dini, Elisabetta Salatelli and Jouko Kankare

- [Multi-phase equation of state of ultrapure hafnium to 120 GPa](#)

L Q Huston, N Velisavljevic, J S Smith et al.

- [EQCM Analysis of the Process of Electrochemical Insertion in Regioregular Alkyl-Substituted Polyterthiophene during n-Doping](#)

Daniilo Dini, Elisabetta Salatelli and Franco Decker



PAPER

Machine learning phases in swarming systems

OPEN ACCESS

RECEIVED
14 October 2022REVISED
30 January 2023ACCEPTED FOR PUBLICATION
28 February 2023PUBLISHED
13 March 2023

Original Content from
this work may be used
under the terms of the
[Creative Commons
Attribution 4.0 licence](#).

Any further distribution
of this work must
maintain attribution to
the author(s) and the title
of the work, journal
citation and DOI.

Tingting Xue^{1,3}, Xu Li^{1,3}, Xiaosong Chen¹, Li Chen^{2,*}  and Zhangang Han^{1,*}¹ School of Systems Science, Beijing Normal University, Beijing 100875, People's Republic of China² School of Physics and Information Technology, Shaanxi Normal University, Xi'an, 710119, People's Republic of China³ Equal contribution.

* Authors to whom any correspondence should be addressed.

E-mail: chenl@snnu.edu.cn and zhan@bnu.edu.cn**Keywords:** phase transitions, collective motion, convolutional neural networks, Vicsek modelSupplementary material for this article is available [online](#)**Abstract**

Recent years have witnessed a growing interest in using machine learning to predict and identify phase transitions (PTs) in various systems. Here we adopt convolutional neural networks (CNNs) to study the PTs of Vicsek model, solving the problem that traditional order parameters are insufficiently able to do. Within the large-scale simulations, there are four phases, and we confirm that all the PTs between two neighboring phases are first-order. We have successfully classified the phase by using CNNs with a high accuracy and identified the PT points, while traditional approaches using various order parameters fail to obtain. These results indicate the great potential of machine learning approach in understanding the complexities in collective behaviors, and in related complex systems in general.

1. Introduction

Swarming systems emerged as a novel class of non-equilibrium systems, in which individual components absorb energy from their surroundings and, in some way, transform it into mechanical work [1–3]. Examples are ubiquitous in nature, ranging from bacteria colonies, animal cells [4–6], bird flocks, to fish schools [7, 8], and human crowds [9, 10]. These systems have been the subject of numerous experimental and theoretical investigations in recent years. Due to the grand challenge in understanding the non-equilibrium nature of swarming systems, several minimal models have been proposed in recent years to capture the physical principles therein [11]. Among them, the Vicsek model is most well-known [12], and has considerably advanced our understanding in the physics behind. It models the swarming population as a group of self-propelled particles, the qualitative change in the collective behaviors is described by the phase transition (PT). The nature of PT of the model, however, was once controversial. The early studies claimed that the PT is similar to an equilibrium continuous transition, but later this conclusion was challenged by large-scale simulations and is confirmed that it is discontinuous, like a liquid-gas transition with phase separation [13, 14]. In fact, there are three rather than simply two phases (ordered and disordered), i.e. the disordered gas-like state, the ordered liquid-like state, and the coexistence of ordered bands and disordered gas due to the density-velocity feedback [15, 16]. More recently, with Eigen microstates approach, reference [17] revealed that the PT in the Vicsek model is essentially a hybrid of continuous and discontinuous PTs, but the discontinuous component dominates as the system size goes infinity. This new perspective well reconciles and terminates the debates.

Interestingly, the latest study [18] identified a fourth phase, i.e. the cross sea phase, in the Vicsek model, which is self-organized, as there is no external driving force. This new phase is not simply a superposition of two band waves, but an independent complex pattern with an inherently selected crossing angle. Therefore, there are four different phases identified in the Vicsek model: the ordered phase, the cross sea phase, the band phase, and the disordered phase so far. Precisely identifying these PT points, however, now becomes extremely challenging.

Identifying PTs is to pin down boundaries between different phases of systems, a fundamental task in understanding the physics of complex systems. Traditionally, the polar order parameter is computed to classify the different phases, which is often useful, e.g. in studying the ordered–disordered phases transition [12]. However, no jump in the average polar order parameter is seen at the transition toward the band-disordered phases, and it is also found insensitive around the cross sea phase [18]. Therefore, other quantities such as the Binder cumulant [15] and the structural order parameter are proposed [18], helping to better distinguish different phases. Nevertheless, it is not *a priori* clear how to properly choose the right order parameters for many non-equilibrium systems without a trial-and-error process. Comparatively, the identification of different phases according to typical snapshots is more accurate, yet this classification approach by human eyes has its limitations when the number of snapshots is huge, and is usually required to precisely determine the regions of different phases [18, 19].

In recent years, machine learning flourishes for its great momentum into almost every branch of science [20–22]. Not surprisingly, machine learning methods have been proposed to study the matter phases [23–25]. The general idea behind several works [26–30] is to use supervised learning; sampling the physical states for several phases, put these labeled configuration information as the training data set to train the neural networks; once the training is completed, the neural networks can be used to estimate the probabilities of testing data that belong to different phases; finally, the PTs can be inferred based on these probabilities. Machine learning is not only very effective in studying PTs in classic models, but also has remarkable ability to reveal various phases of matter in quantum many-body systems [31–34]. Current studies indicate its great potential in identifying PTs in complex systems, for its extraordinary advantages over traditional methods.

In this work, we employ the convolutional neural network (CNN) [22, 26, 35] to classify different phases in Vicsek model according to the sampled snapshots. By large-scale simulations of Vicsek model, we first numerically confirm that all PTs in each of the two neighboring phases are first-order. By adopting various order parameters to analyze the PTs, we find that the boundaries for different phases are fuzzy due to the insensitivity of these order parameters, and even the types of PTs cannot be determined. In contrast, the supervised learning based on CNNs conquers these difficulties, which successfully classifies all four phases. The precision of phase classification is robust to the choice of order parameters.

2. The model

In the standard Vicsek model [12], N self-propelled particles with a constant velocity v_0 that move in a two-dimensional domain of size $L \times L$ with the periodic boundary condition. They move synchronously at discrete time steps by a fixed distance $v_0 \Delta t$. Each particle i is endowed with an angle θ_i that determines the movement direction. Its update is determined by the average orientations of its neighbors (defined as particles within a circle of radius $R = 1$ centered around particle i , including itself) plus some noise. Specifically,

$$\theta_i(t + \Delta t) = \Theta \left[\sum_{j: d_{ij} < R} \mathbf{v}_j(t) \right] + \eta \xi_i(t), \quad (1)$$

where $\Theta[\mathbf{v}]$ represents the angle that describes the direction of the two dimensional vector \mathbf{v} and d_{ij} is the distance between particle i and j . The noise ξ_i is chosen from the uniform distribution within the interval $[-1/2, 1/2]$, and η is the noise amplitude. In our study, the density $\rho = 0.5$ and $v_0 = 1.0$ are fixed throughout the study.

3. Results and analysis

We first report typical snapshots in figure 1 to provide the overall picture for the Vicsek model when the noise is varied. For small noise, the ordered phase is seen in figure 1(I). Increasing noise leads to the cross sea phase (figure 1(III)), where the interactions become more intensive for the cluster characteristics. With further increase in noise amplitude η , the band structure could emerge (figure 1(V)), which is locally ordered and of high density. Finally, the system evolves into the disordered phase when the noise becomes very strong, see figure 1(VII). However, we find that the phase boundaries are not distinct, bistable states are always seen for each two neighboring phases. For example, snapshots in figure 1(II) show the coexistence of ordered and cross sea phases, where the two phases interchange into each other from time to time. Similar observations are made between the cross sea and the band phase (figure 1(IV)), and also between the band phase and the disordered phase (figure 1(VI)). Here, the bistability and the phase coexistence in figure 1(VI)

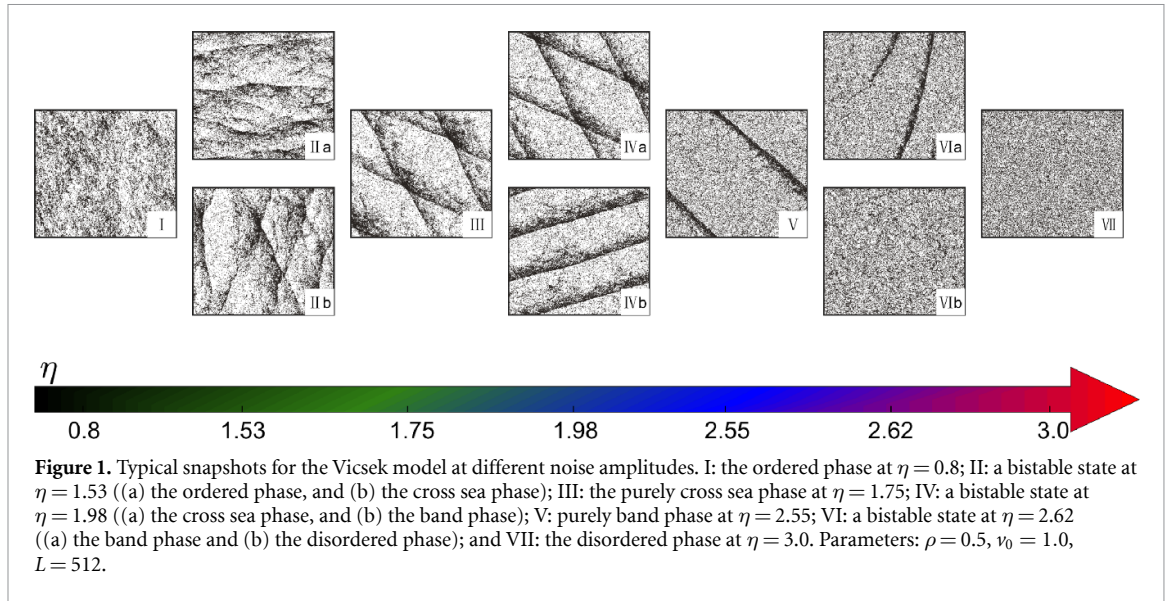


Figure 1. Typical snapshots for the Vicsek model at different noise amplitudes. I: the ordered phase at $\eta = 0.8$; II: a bistable state at $\eta = 1.53$ ((a) the ordered phase, and (b) the cross sea phase); III: the purely cross sea phase at $\eta = 1.75$; IV: a bistable state at $\eta = 1.98$ ((a) the cross sea phase, and (b) the band phase); V: purely band phase at $\eta = 2.55$; VI: a bistable state at $\eta = 2.62$ ((a) the band phase and (b) the disordered phase); and VII: the disordered phase at $\eta = 3.0$. Parameters: $\rho = 0.5$, $v_0 = 1.0$, $L = 512$.

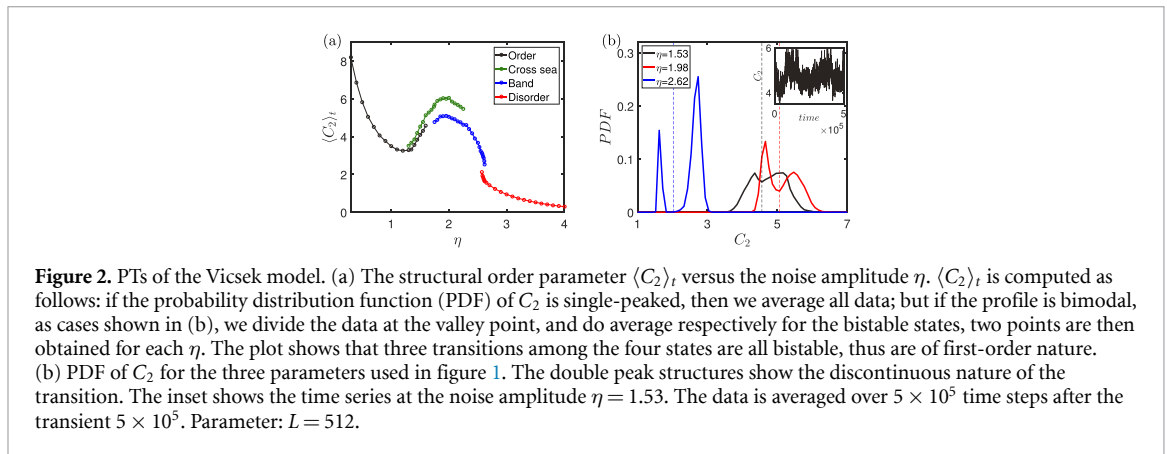


Figure 2. PTs of the Vicsek model. (a) The structural order parameter $\langle C_2 \rangle_t$ versus the noise amplitude η . $\langle C_2 \rangle_t$ is computed as follows: if the probability distribution function (PDF) of C_2 is single-peaked, then we average all data; but if the profile is bimodal, as cases shown in (b), we divide the data at the valley point, and do average respectively for the bistable states, two points are then obtained for each η . The plot shows that three transitions among the four states are all bistable, thus are of first-order nature. (b) PDF of C_2 for the three parameters used in figure 1. The double peak structures show the discontinuous nature of the transition. The inset shows the time series at the noise amplitude $\eta = 1.53$. The data is averaged over 5×10^5 time steps after the transient 5×10^5 . Parameter: $L = 512$.

are confirmed in previous studies [15], which is a first-order PT; the nature of other two transitions (from I to III, III to V), to our best knowledge, have not yet been confirmed.

Because of the insensitivity of the polar order parameter to the PT, especially around the cross sea and band phases, here we adopt the structure order parameter C_2 [18, 19] as our new order parameter. It is a local integral over the two particle correlation function formally given by

$$C_2 = \left(\frac{N}{L^2}\right)^2 \int_{R^2} [g(|\mathbf{r}_1 - \mathbf{r}_2|) - 1] \times \theta(R - |\mathbf{r}_1|)\theta(R - |\mathbf{r}_2|) d\mathbf{r}_1 d\mathbf{r}_2, \tag{2}$$

where θ is the Heaviside function, $g(r)$ is the usual pair correlation function. The value is zero for the independent particle ensemble, and becomes large when particles are clustered. Therefore, C_2 works generally better than the traditional polar order parameter and the Binder cumulant for its ability in capturing the structural change. A simple way of computing C_2 is given in section I of SM.

Figure 2(a) shows the dependence of the average structure order parameter C_2 on the noise amplitude, where two scenarios are seen. While a single value of C_2 corresponds to a pure state (e.g. figure 1(I, III, V, VII)), the two-value cases are for the bistable states (figure 1(II, IV, V I)). We can see that the bistability is observed for all three transitions among four pure states, indicating first-order PTs. And this observation is strengthened by the bimodal PDF as well as the time series, see figure 2(b).

We also compare the structure order parameter C_2 with the traditional polar order parameter, and find that C_2 indeed has advantage in distinguishing the cross sea phase (for details see section II of SM). Still, the change in C_2 is very small in some certain bistable states, or the system is prone to stabilize into a state within the bistable region with a little chance to evolve into the other due to the deep potential well. All these factors

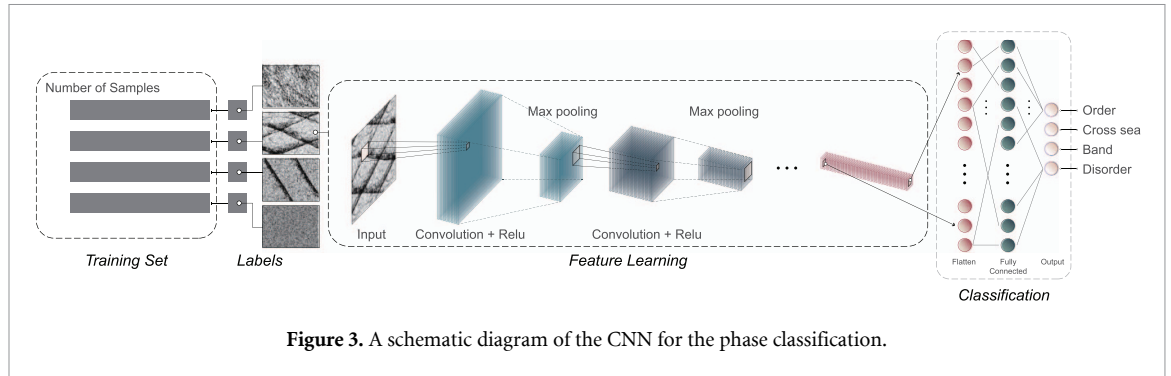


Figure 3. A schematic diagram of the CNN for the phase classification.

lead to great difficulties in the phase segmentation. In addition, both order parameters are greatly influenced by the system size, and the cross sea and band state are absent when the system is small (see section III of SM).

4. Convolutional neural network

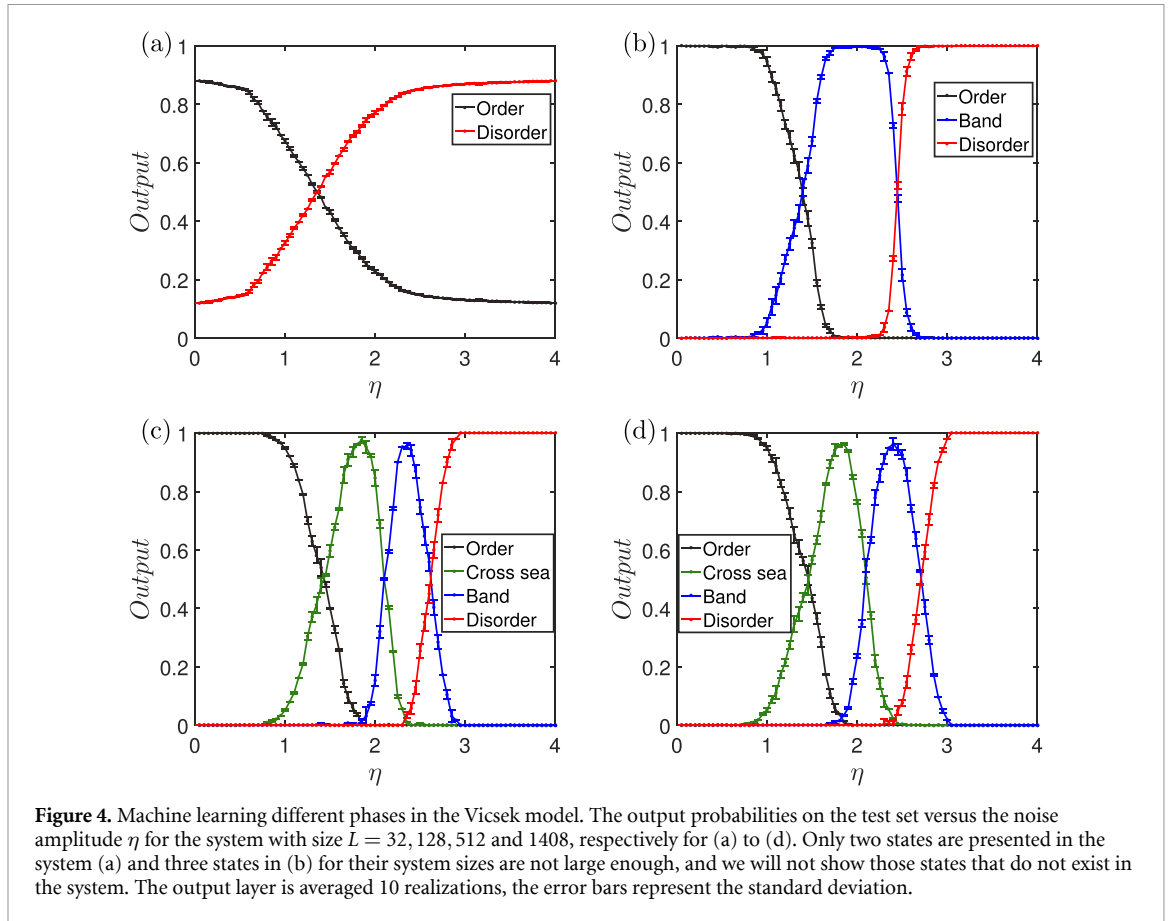
We now turn to adopt CNNs to classify the rich phases of Vicsek model with the help of PyTorch [36]. The particle configuration is sampled as an image, and the task turns to be the image classification. The method belongs to the supervised learning that tries to find the correct mapping between the configuration and the phase label. Figure 3 shows the network structure of the CNN. It is composed of an input layer with the same size as the image pixel sampled, multiple cascaded convolution-pooling layers, fully connected layers, and the output layer [37, 38]. Each convolution-pooling stage is a series of the convolution layer to extract a feature map and the max-pooling layer to reduce the feature map size. We use zero padding to maintain the spatial dimensions of feature maps during the convolution processes [35, 38]. To avoid the vanishing gradient problem during training, we use the rectified linear unit activation for each layer of CNN. We utilize the stochastic gradient descent optimization function in the learning rate for stable convergence [39]. The output layer contains nodes with number equal to the number of classes, the softmax function is adopted as the activation function to yield the probabilities as the prediction for each class.

In our work, we use three independent datasets: the training, validation, and test sets. To prepare the image datasets, we obey the following procedure. For the chosen noise strength η and system size $L \times L$, the snapshot of particle configuration (i.e. the two coordinates (x, y) as a dot for all N particles) is sampled as an output image, the original resolution is of 1167×875 pixels in RGB format. The images are then reduced into 512×512 . Since we use periodic boundary condition in the Vicsek model, there is no preferred direction, the movement is isotropic and has the translational and rotational invariances.

The training and validation sets are sampled in the four pure states to guarantee the correctness for the assigned label for each image. Since the samples are within the pure state instead of the bistable region, there is little ambiguity for labeling states, because we are explicitly aware of what state it is at that noise strength. This is the criterion to assign the label. The test set is prepared across the whole parameter domain of noise strength without label. The number of images in three datasets for different system sizes are listed in table I in SM, e.g. the dataset sizes are 12 000, 4800 and 103 200 respectively for training, validation, and test sets when $L = 512$. For details about CNNs and the data sets, see section IV of SM.

The whole training process consists of two stages. In the first stage, in each epoch the CNN is fed with all training data, and then we validate the CNN with the validation set to monitor its performance and stability. By validation, we find the CNNs are able to classify different phases successfully, the accuracy is almost 100% when the system size is not very large. This is beyond our expectation because when the system is small, the snapshots are difficult to distinguish artificially by eyes. When the system becomes large, the CNN still can classify the ordered, cross sea, band and disordered phases. Though the accuracy now decreases to around 86.2%. This is because the correctness of labels in the training datasets cannot be guaranteed due to the narrow regions for the newly emerging phases, thus leads to the accuracy decrease on the validation set. For more details, see section IV of SM.

For further evaluation, we also compute the corresponding confusion matrix and F1-score [40]. The advantage of the confusion matrix is that it can provide more details about the classification, e.g. we can see which samples are more likely to be incorrectly classified into which one. Specifically, we find that the accuracy decrease in large systems is mainly because the band phase is wrongly classified into the ordered state, and the cross sea phase is likely to be misclassified into either ordered or band phase, see figure S10 in SM. Based upon the confusion matrix, the F1-score is computed respectively for the four phases and for nine system sizes, see table II in SM. In line with the trend of accuracy, the F1-scores decrease from 1 and stabilizes



around $0.81 \sim 0.84$ as L increases. But this score keeps at high values for disordered phases, meaning this phase is more easily to be distinguished and is much less influenced by the system size, consistent with the observations in the confusion matrix.

After the training is completed, we enter into the second stage, use the trained CNNs to classify the images in the test data set. The output probabilities for the available phases on the test set as a function of the noise for four different system sizes are shown in figure 4. Notice that for systems with not large enough size, the cross sea state and even band state are absent. By definition, the output probability is supposed to be unity or zero in the pure state, but could be any number between the two extremes in the bistable region. Take figure 4(c) for example, when the noise strength η increases from zero, the output probability is predicted to be 100% within the ordered state; as $\eta \gtrsim 1$ this predicted probability gradually becomes smaller, and the probability within the cross sea state starts to increase, since the system goes through a bistable region. When $\eta \approx 1.75$, the bistable region between these two phases terminates because the two probabilities now go to be nearly zero and unity. Note that, the continuous shapes in the output probabilities do not mean continuous PTs because the output probabilities capture the probabilities of the two involved phases in the bistable region, the PTs of swarming behaviors in the Vicsek model are all first-order PTs.

Given these probabilities, their intersections can naturally interpreted as the transition point of two neighboring phases, since the probabilities there are approximately 50%. With this idea, we estimate $\eta_{c1} \approx 1.47$, $\eta_{c2} \approx 2.11$, $\eta_{c3} \approx 2.58$ in figure 4(c), all fall within the bistable regions. Strictly speaking, there is no single clear-cut single threshold in the first-order PTs, the boundary for two neighboring phases is a parameter interval defined by two thresholds. But these two thresholds are difficult to infer precisely. Therefore, here we instead provides a single estimated threshold that approximately divide the two phase regions.

5. Conclusions

Alongside the previous concerns, here we aim to clarify the nature of all PTs in the Vicsek model. By adopting the structural order parameter [18] and the technique of PDF segmentation [16], we confirm that all PTs between the two neighboring phase are first-order given the system is large enough. The existing problem is that the structural order parameter is still insensitive to the parameter change in some regions that makes the

PDF segmentation bad and thus less precise in characterizing the PTs. Therefore, we use the CNNs to classify different phases by feeding them labeled snapshot images. We find that this approach is able to successfully carry out phase classification with high accuracies. The transition points of two neighboring phases can also be inferred accordingly.

Our approach is feature extraction from raw data within different states, which not only correctly classifies the given states into different phases, but also infers PT points as well. This work opens up new possibilities for exploring PTs in systems where *a priori* knowledge is unavailable, thus the proper order parameter is unknown. Given the success [33, 41, 42] in complex networks, materials science, quantum systems etc we look forward to applying machine learning to detect, predict and identify PTs in swarming systems and in many other non-equilibrium fields in the future.

Data availability statement

All data that support the findings of this study are included within the article (and any supplementary files).

Acknowledgments

We acknowledge Weiran Cai (Soochow University) and Jiqiang Zhang (Ningxia University) for helpful comments. Zhangang Han and Tingting Xue are supported by the National Natural Science Foundation of China under Grant No. 62176022. Xiaosong Chen and Xu Li are supported by the National Natural Science Foundation of China under Grant No. 12135003. Li Chen is supported by the National Natural Science Foundation of China under Grant No. 12075144.

ORCID iD

Li Chen  <https://orcid.org/0000-0002-0335-466X>

References

- [1] Netzer G, Yarom Y and Ariel G 2019 *Physica A* **530** 121550
- [2] Marchetti M C, Joanny J-F, Ramaswamy S, Liverpool T B, Prost J, Rao M and Simha R A 2013 *Rev. Mod. Phys.* **85** 1143
- [3] Ramaswamy S 2017 *J. Stat. Mech.* **054002**
- [4] Wu X-L and Libchaber A 2000 *Phys. Rev. Lett.* **84** 3017
- [5] Elgeti J, Winkler R G and Gompper G 2015 *Rep. Prog. Phys.* **78** 056601
- [6] Prost J, Jülicher F and Joanny J-F 2015 *Nat. Phys.* **11** 111
- [7] Cavagna A and Giardina I 2014 *Annu. Rev. Condens. Matter Phys.* **5** 183
- [8] Calovi D S, Lopez U, Ngo S, Sire C, Chaté H and Theraulaz G 2014 *New J. Phys.* **16** 015026
- [9] Bottinelli A, Sumpter D T and Silverberg J L 2016 *Phys. Rev. Lett.* **117** 228301
- [10] Bain N and Bartolo D 2019 *Science* **363** 46
- [11] Shaebani M R, Wysocki A, Winkler R G, Gompper G and Rieger H 2020 *Nat. Rev. Phys.* **2** 181
- [12] Vicsek T, Czirók A, Ben-Jacob E, Cohen I and Shochet O 1995 *Phys. Rev. Lett.* **75** 1226
- [13] Solon A P, Chaté H and Tailleur J 2015a *Phys. Rev. Lett.* **114** 068101
- [14] Solon A P, Caussin J-B, Bartolo D, Chaté H and Tailleur J 2015b *Phys. Rev. E* **92** 062111
- [15] Chaté H, Ginelli F, Grégoire G and Raynaud F 2008 *Phys. Rev. E* **77** 046113
- [16] Xue T, Li X, Grassberger P and Chen L 2020 *Phys. Rev. Res.* **2** 042017
- [17] Li X, Xue T, Sun Y, Fan J, Li H, Liu M, Han Z, Di Z and Chen X 2021 *Chin. Phys. B* **30** 128703
- [18] Kürsten R and Ihle T 2020 *Phys. Rev. Lett.* **125** 188003
- [19] Kürsten R, Stroteich S, Hernández M Z and Ihle T 2020 *Phys. Rev. Lett.* **124** 088002
- [20] von Lilienfeld O A and Burke K 2020 *Nat. Commun.* **11** 1
- [21] Jones N 2017 *Nature* **548** 379
- [22] Carleo G, Cirac I, Cranmer K, Daudet L, Schuld M, Tishby N, Vogt-Maranto L and Zdeborová L 2019 *Rev. Mod. Phys.* **91** 045002
- [23] Jordan M I and Mitchell T M 2015 *Science* **349** 255
- [24] Van Nieuwenburg E P, Liu Y-H and Huber S D 2017 *Nat. Phys.* **13** 435
- [25] Venderley J, Khemani V and Kim E-A 2018 *Phys. Rev. Lett.* **120** 257204
- [26] Carrasquilla J and Melko R G 2017 *Nat. Phys.* **13** 431
- [27] Deng D-L, Li X and Sarma S D 2017 *Phys. Rev. X* **7** 021021
- [28] Rodríguez-Nieva J F and Scheurer M S 2019 *Nat. Phys.* **15** 790
- [29] Wetzel S J 2017 *Phys. Rev. E* **96** 022140
- [30] Zhang W, Liu J and Wei T-C 2019 *Phys. Rev. E* **99** 032142
- [31] Torlai G and Melko R G 2018 *Phys. Rev. Lett.* **120** 240503
- [32] Ch'Ng K, Carrasquilla J, Melko R G and Khatami E 2017 *Phys. Rev. X* **7** 031038
- [33] Rem B S, Käming N, Tarnowski M, Asteria L, Fläschner N, Becker C, Sengstock K and Weitenberg C 2019 *Nat. Phys.* **15** 917
- [34] Carleo G and Troyer M 2017 *Science* **355** 602
- [35] Krizhevsky A, Sutskever I and Hinton G E 2012 *Advances in Neural Information Processing Systems* vol 25
- [36] Paszke A et al 2019 *Advances in Neural Information Processing Systems* vol 32

- [37] LeCun Y, Bengio Y and Hinton G 2015 *Nature* **521** 436
- [38] Goodfellow I, Bengio Y and Courville A 2016 *Deep Learning* (Cambridge, MA: MIT press)
- [39] Shalev-Shwartz S and Zhang T 2013 *J. Mach. Learn. Res.* **14** 567–99
- [40] Sammut C and Webb G I 2011 *Encyclopedia of Machine Learning* (New York: Springer)
- [41] Ni Q, Tang M, Liu Y and Lai Y-C 2019 *Phys. Rev. E* **100** 052312
- [42] Li H, Jin Y, Jiang Y and Chen J Z 2021 *Proc. Natl Acad. Sci.* **118** e2017392118